

# Development of a Symmetric Ring Junction as Four-Port Reflectometer for Complex Reflection Coefficient Measurements

Kim Yee LEE<sup>1</sup>, Boon Kuan CHUNG<sup>1</sup>, Kok Yeow YOU<sup>2</sup>, Ee Meng CHENG<sup>3</sup>, Zulkifly ABBAS<sup>4</sup>

<sup>1</sup> Dept. of Electrical and Electronic Engineering, Universiti Tunku Abdul Rahman, 43000, Selangor, Malaysia

<sup>2</sup> Dept. of Radio Communication Engineering, Universiti Teknologi Malaysia, 81310 UTM, Skudai, Johor, Malaysia

<sup>3</sup> School of Mechatronic Engineering, University Malaysia Perlis, Ulu Pauh Campus, 02600 Arau, Perlis, Malaysia

<sup>4</sup> Dept. of Physics, Universiti Putra Malaysia, UPM Serdang 43300, Malaysia

kylee@utar.edu.my, chungbk@utar.edu.my, kyyou@fke.utm.my, emcheng@unimap.edu.my, za@science.upm.edu.my

**Abstract.** Six-port reflectometer is well-known for its ability to measure magnitude and phase-shift of microwave signal using four power detectors that perform magnitude-only measurements. This paper presents the development of an innovative symmetric ring junction as four-port reflectometer for complex reflection coefficient measurements. It reduces the number of required detectors to two. Design optimization, new calibration modeling and algorithm are discussed in details for this four-port reflectometer. The developed four-port reflectometer is compared to five-port reflectometer and vector network analyzer. It is found that the measured magnitude and phase-shift show good performance in comparison with the commercial vector network analyzer and the five-port reflectometer.

## Keywords

Six-port reflectometer, complex reflection coefficient, four-port reflectometer, network analysis, nonlinear multi-objective optimization

## 1. Introduction

Complex reflection coefficient that contains both magnitude and phase-shift information is very useful in many microwave measurements. Obtaining the phase-shift information is a major challenge that requires expensive circuitry, particularly for high frequencies [1–2]. Accurate, easy to operate, low cost, low computational time, compact and simple circuitry were some of the primary concerns. Beside the advanced and sophisticated vector network analyzer (VNA), six-port reflectometer (SPR) remains as one of the popular alternative because of its simple circuitry and operations.

For decades, many articles on SPR have been published since the first paper by Engen [3] in 1977. Beside the general laboratory measurements, there are broad usages of SPR for example in high power measurements [4],

portable material measurements [5], wireless applications and many more [6], [7].

Generally, SPR detects three different phase-shift positions of a reflected signal and uses six-port's formulas to convert them into three circle radius. The intersection of those three circles leads to the unknown complex reflection coefficient [4]. Calibration procedure is required in a SPR for accurate determination of reflection coefficient. Some of the limits and accuracy improvement has been discussed in [8], [9]. Besides, additional statistical methods can be used to get more accurate results in a SPR [10].

A common SPR required six ports, namely the source port, test port, and four detection ports. For a stable source, a modified PC-based SPR [5], [11] named five-port reflectometer (5PR) reduced the number of detection ports from four to three. The reduction of detection ports reduced the cost for SPR. Theoretically, it is possible to determine the unknown magnitude and phase-shift using two detection ports. Hence, realizing the concept will minimize the required components and further reduce the cost of SPR. In a series of publications by Haddadi [12–16], he proved that the SPR using two detection ports or so called four-port reflectometer (FPR) is workable. Although the FPR is very attractive in terms of minimum detection ports, unfortunately it was constructed with 6 Wilkinson power dividers and a 90° delay line [13]. In addition, eight standards were required for the FPR calibration. A higher order FPR equations [13] were formulated due to a hard compromise between the frequency range of operation and the expected measurement accuracy that drives the FPR. This resulted in complicated inverse equations that were inefficient for computational algorithm and measurement process. Hence, a simpler structure and algorithm of FPR is innovated to optimize the concept and practicality of the FPR. Furthermore, reduction of the number of calibration standard will be an added advantage for operation of FPR if the required measurement accuracy can be maintained.

For an accurate reflection coefficient calculation in FPR, a very close initial value of phase-shift is necessary

[8] or by implementing the evolutionary multi-objective optimization algorithm [17]. The former is somehow not an easy task while the multi-objective optimization algorithm requires huge computational time. In this work, the equations of 5PR [5], [11] are modified to model a simple yet accurate FPR. The new FPR model incorporated both the ideas [8], [17] by creating a close initial value and a single-objective optimization equation to refine and solve the multi-objective optimization problem in FPR. Besides, modification of the existing 5PR structure [5] to become FPR is investigated in details. Simulation results for both the 5PR and FPR using AWR Microwave Office (MWO) are studied. The algorithm programmed using MATLAB is created and tested. Finally, the performances of the FPR and 5PR are compared with commercial VNA for measurements of several unknown samples.

## 2. Modeling and Calibration

The magnitude  $|\Gamma|$  and phase-shift  $\theta$  of a  $90^\circ$  delay line in a FPR are analytically related to the detectors' DC voltages  $V_i$  as [13]

$$V_i = \frac{P_0}{8} \left( 1 + \frac{|\Gamma|^2}{4} - |\Gamma| \sin \theta_i \right) \quad (1)$$

where  $i$  is the port number ( $i = 3$  and  $4$ ). A stable source with known power  $P_0$  is expected for an ideal FPR; otherwise a reference port to measure  $P_0$  is necessary. However, for a single frequency source that is implemented in a fixed measurement structure, the absolute value of  $P_0$  is not needed.

For a general FPR structure, equation (1) can be rewritten in the form of

$$V_i = x_i (y_i^2 + |\Gamma|^2 - 2y_i |\Gamma| \sin \theta_i). \quad (2)$$

The phase-shift independent term  $y_i^2 + |\Gamma|^2$  in (2) represents the center value of the detected signal, whereas the term  $-2y_i |\Gamma| \sin \theta_i$  shows the signal variation for different locations of phase-shift on the delay line. The  $x_i$  and  $y_i$  are constants that can be determined through a calibration procedure.

To get a close initial value of phase-shift  $\theta$ , equation (2) is expressed in the form of

$$\frac{V_i}{x_i} = y_i^2 + |\Gamma| - 2y_i |\Gamma| \sin \theta_i - E \quad (3)$$

$$\text{where} \quad E = |\Gamma| - |\Gamma|^2. \quad (4)$$

A close initial value can be obtained when  $E \approx 0$ , that is, when  $|\Gamma|$  is close to 1 or 0. Otherwise,  $E$  will vary with the value of  $|\Gamma|$ . It can be up to a maximum of 0.25 when  $|\Gamma| = 0.5$ .

For computational algorithm, a proper optimization equation is required. A system of equation (3) in FPR for

$i = 3, 4$  can be formed by assuming  $\theta_3 = \theta$  and  $\theta_4 = \theta + \varphi$  as

$$\frac{V_3}{x_3} - y_3^2 + E = |\Gamma| (1 - 2y_3 \sin \theta), \quad (5)$$

$$\frac{V_4}{x_4} - y_4^2 + E = |\Gamma| (1 - 2y_4 \sin(\theta + \varphi)) \quad (6)$$

where  $\varphi$  is the phase-shift delay between detection port 3 and port 4. Based on (5) and (6), the advantage of the model is it does not limit the phase-shift delay in FPR to  $90^\circ$  as in [13].

By dividing (5) with (6), a single-objective optimization equation is formed.

$$\left( \frac{V_3}{x_3} - y_3^2 + E \right) (1 - 2y_4 \sin(\theta + \varphi)) - \left( \frac{V_4}{x_4} - y_4^2 + E \right) (1 - 2y_3 \sin(\theta)) = 0 \quad (7)$$

Solving (7) with a set of  $E$  from 0 to 0.25 leads to the unknown phase-shift  $\theta$ . Fitness analysis can be performed to identify the right set of  $E$  and the unknown phase-shift  $\theta$ . The magnitude  $|\Gamma|$  can be calculated by

$$|\Gamma| = \frac{\frac{V_3}{x_3} - \frac{V_4}{x_4} - y_3^2 + y_4^2}{2(y_3 \sin(\theta) - y_4 \sin(\theta + \varphi))}. \quad (8)$$

The nonlinear multi-objective optimization model in FRP is transformed into a new single-objective model as shown in (7) and (8). The model can be solved easily by a classical optimization method.

For calibration, the constants  $x_i$  and  $y_i$  in (3) are determined. There is no limitation on what calibration standards should be used. In this work the calibration was carried out using a *match* load, an *open* and a *short*. Substituting  $|\Gamma| = 0$  for a *match* calibration standard ( $50 \Omega$  load) into (3) yields

$$y_i = \sqrt{\frac{V_{i\_match}}{x_i}} \quad (9)$$

for  $i = 3$  and  $4$ . By choosing the *open* standard as  $|\Gamma| = 1$  and  $\theta_{open} = 0$ , the *short* standard as  $|\Gamma| = 1$  and  $\theta_{short} = 180$ , equation (3) becomes

$$\frac{V_{i\_open}}{x_i} = \frac{V_{i\_short}}{x_i} = 1 - 2y_i^2 \sin \theta_i. \quad (10)$$

The mean of equation (10) formulated for the *short* and *open* is taken and substituted into (8) to form a single-objective optimization equation.

$$\frac{V_{i\_open} + V_{i\_short} - 2V_{i\_match}}{2} - \left( x_i - 2\sqrt{x_i V_{i\_match}} \sin \theta_i \right) = 0 \quad (11)$$

for  $i = 3$  and  $4$ .

### 3. Computer Algorithm

The computer algorithm starts with the process of calibration using three calibration standards. This is followed by solving the single-objective optimization problem in FPR. Since there are numerous possible values of  $E$ , hence all  $E$  from 0 to 0.25 are applied for the fitness analysis to obtain the best optimized magnitude and phase-shift.

The algorithm is programmed using MATLAB. It comprises two major parts which are calibration and measurement as illustrated in the flow chart of Fig. 1. In the calibration, the constants  $x_i$  and  $y_i$  are determined using (9) and (11). The constant  $x_i$  is calculated by optimizing (11) using the MATLAB build-in function *fzero*. The command *fzero* is a root finder of a nonlinear function that uses a combination of bisection, secant, and inverse quadratic interpolation. Since equation (9) consists of two possible  $y_i$ , both set of answers must be used for the best selection analysis later. For the measurement in this work, the phase-shift is obtained by optimizing (7) using the *fzero* function. The respective magnitude is then calculated using (8).

Equation (2) is used to examine the fitness of optimized magnitude and phase-shift. For an ideal case, the optimized magnitude and phase-shift should fit equation (2) without error. In this work, the selection of best magnitude and phase-shift is based on minimum total error of port 3 and 4. In the algorithm, the selected magnitude and phase-shift should be a correct solution if the criterion is

met which in this work the error is set to be less than 0.0001. The criterion of 0.0001 in the algorithm is equivalent to less than 0.01% error for both the calculated magnitude and phase-shift. Otherwise, the process will be repeated for another set of  $E$ . One set of correct answers should be laid within the  $E$  values of 0 to 0.25. If no solution meets the criterion, error of all calculations will be dissected. The best set of phase-shift and magnitude with minimum total error will be selected. Selection of incremental value for  $E$  in the algorithm determines the accuracy and calculation time. From this study, an increment of 0.001 is sufficient to get an accurate answer in less than 1 second computational time. The increment of  $E = 0.001$ , carries the meaning of providing 251 data sets for the best fit selection. In this work,  $E = 0.001$  gives saturated errors of 0.0280 in magnitude and  $1.611^\circ$  in phase-shift. Although greater data sets can be obtained by selecting smaller increment of  $E$ , it requires longer calculation time.

In addition to all the above, error correction must be executed to the selected best solution. The correction is done by comparing the optimized solution to the calibration standards'  $\theta$  and  $|\Gamma|$ . This correction is particularly important for phase-shift since the assumption of  $\theta_3 = \theta$  and  $\theta_4 = \theta + \varphi$  were made initially. The proposed algorithm is much simpler than [13].

### 4. Design and Methodology

First, the model of FPR and 5PR are examined. Microwave Office (MWO) is used to simulate the configuration of FPR and 5PR [5] as shown in Fig. 2. Considering that all results are critically dependent on signal source power stability and dynamic range of the detectors, the design was focused on a single frequency.

It is a simple symmetric five-port ring junction that operated at 2 GHz [5]. Each port is designed to be separated with a magnitude of 0.5 and phase-shift delay of  $120^\circ$  to the ports next to it. A custom made (imperfect) symmetric ring junction and perfect detectors are used in the simulation. The purpose of the simulation is to investigate the propagated error of the custom made symmetric ring junction as FRP. If a perfect symmetric ring junction and perfect detectors are being applied, no error will be detected. In this work, port 1 and port 2 are set as source and testing port respectively. S-parameters of port 3 to port 5 ( $S_{31}$ ,  $S_{41}$  and  $S_{51}$ ) are simulated with several known standards that are connected to port 2. For 5PR, the S-parameters of all three detection ports ( $S_{31}$ ,  $S_{41}$  and  $S_{51}$ ) are applied to calculate the magnitude and phase-shift. An algorithm similar to [5] is programmed using MATLAB for 5PR. Whereas for FPR, only the data from port 3 and port 4 ( $S_{31}$  and  $S_{41}$ ) are used. Since port 5 is properly terminated with  $50 \Omega$ , it can be considered matched and ignored in FPR. Hence, the simulation data for 5PR can be used at the same time for FPR. The  $\varphi$  in (7) is replaced by a measurement's value of VNA in this work. The  $|\Gamma|$  magnitudes of 0, 0.1, 0.5, and 1

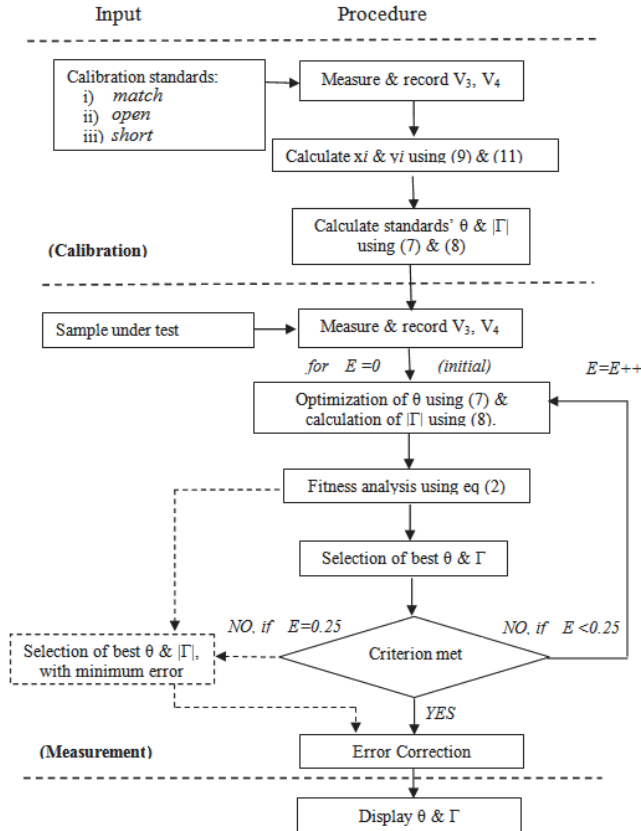


Fig. 1. Flow chart of computer algorithm programmed using MATLAB.

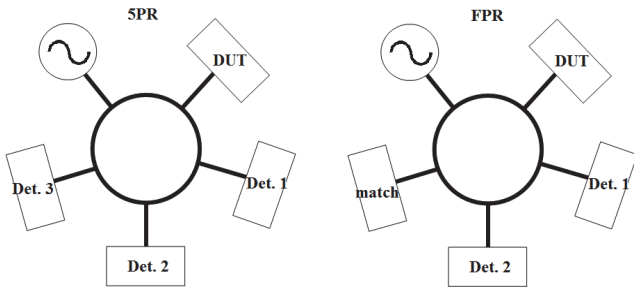


Fig. 2. Configuration of 5PR and FPR.

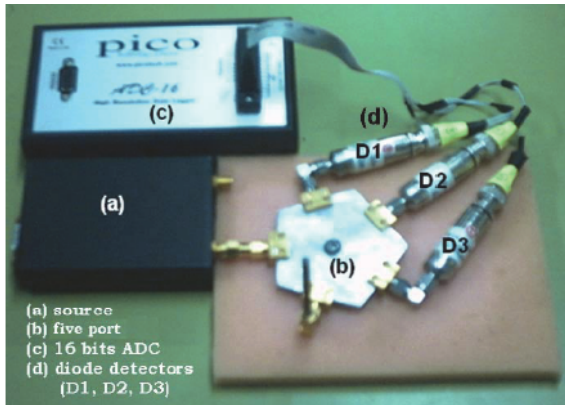


Fig. 3. Measurement setup of Five-port [5] and Four-port reflectometer.

are chosen to cover all the typical cases in the reflection coefficient measurements. Different phases-shifts are tested and the data are analyzed by the respective algorithms.

Secondly, the symmetric ring junction of FPR and 5PR is fabricated. The measurement setup is as illustrated in Fig. 3 [5], which the details can be found in [5]. Measurements are performed using several unknown samples. All three detection ports will be used for 5PR, whereas only port 3 and port 4 are applied for FPR. Since port 5 is connected to a 50 Ω diode detector, it can be considered as matched. Hence, modification of 5PR measurement setup is unnecessary in FPR measurement. The same set of detected voltages for 5PR and FPR will be recorded and analyzed by MATLAB algorithms respectively. They are both tested and compared to HP8720 VNA for verification.

### 5. Results and Discussions

The calculated results using MWO simulation are as shown in Fig. 4 and Fig. 5 for magnitude and phase-shift, respectively. The results of 5PR and FPR are in good agreement for calculation of magnitudes and phase-shifts. Since all the results have been obtained by simulation, the errors should actually be practically zero. Non-zero errors are indication of the imperfection of the designed symmetric ring junction and its effect to the computational algorithm.

For further analysis, the error of each calculation is scrutinized. The magnitude errors are shown in Fig. 6. Overall, the errors for 5PR and FPR are within the satisfac-

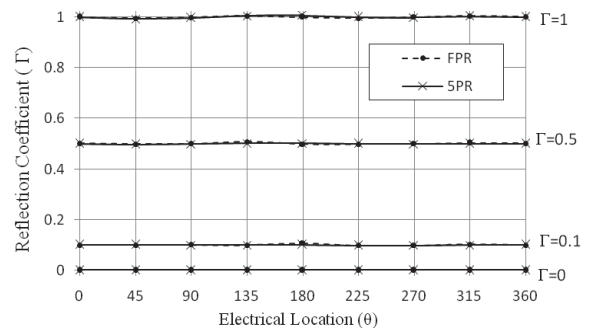


Fig. 4. Comparison of calculated magnitudes.

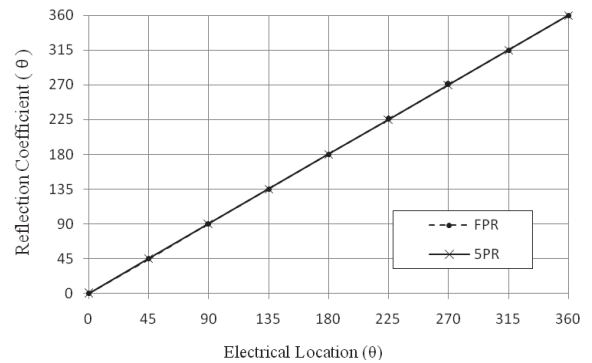
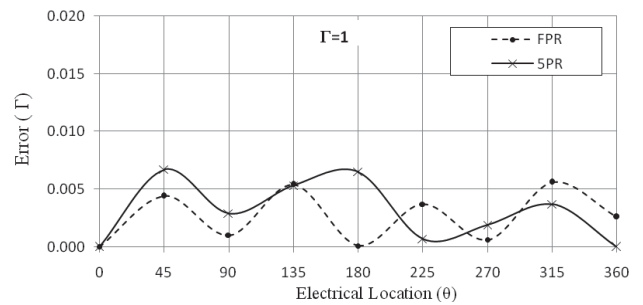
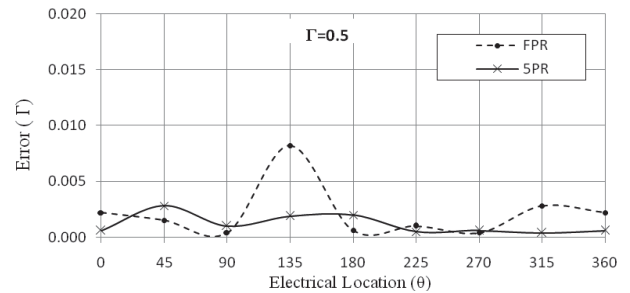


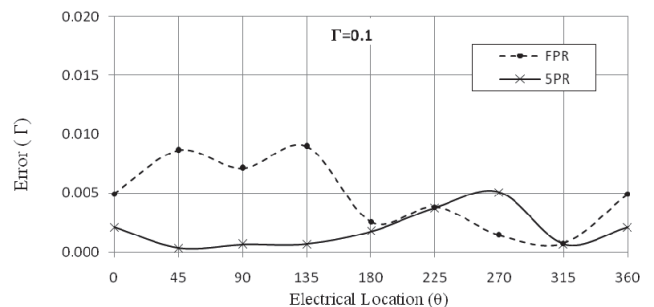
Fig. 5. Comparison of calculated phase-shifts.



(a) For magnitude of  $\Gamma=1$ .



(b) For magnitude of  $\Gamma=0.5$ .



(c) For magnitude of  $\Gamma=0.1$ .

Fig. 6. Comparison of error in calculated magnitudes.

tory range. The errors of FPR are higher than 5PR when measuring low  $\Gamma$ . This is anticipated in FPR due to the use of less detection ports. The error is also contributed by the FPR computational algorithm. The FPR produces a maximum error of 0.0082 at  $\Gamma = 0.5$ , and 0.0081 for  $\Gamma = 0.1$ . This shows that FPR is able to attain a magnitude error of less than 0.010.

The phase-shift errors are as shown in Fig. 7. FPR is found to be in good agreement with 5PR especially for  $\Gamma = 1$  and  $\Gamma = 0.5$ . It shows that lower reflection coefficient causes higher error in phase-shift measurement. The errors of FPR are slightly higher than 5PR. It is similarly due to the use of less detection ports in an imperfect symmetric ring junction and partly due to the computational algorithm. At  $\Gamma = 0.1$ , FPR has a maximum error of  $2.39^\circ$  whereas 5PR has a maximum error of  $0.65^\circ$ .

Measurements of several unknown standards are performed using FPR, 5PR and VNA. The results are as listed in Tab. 1. The data indicate a close similarity with theoretical analyses in the first part, which shows that FPR is able to measure both magnitude and phase-shift accurately. From Tab. 2, the maximum error of FPR is 0.0241 and  $2.95^\circ$  for magnitude and phase-shift, respectively. This proves that FPR is able to provide comparable performance

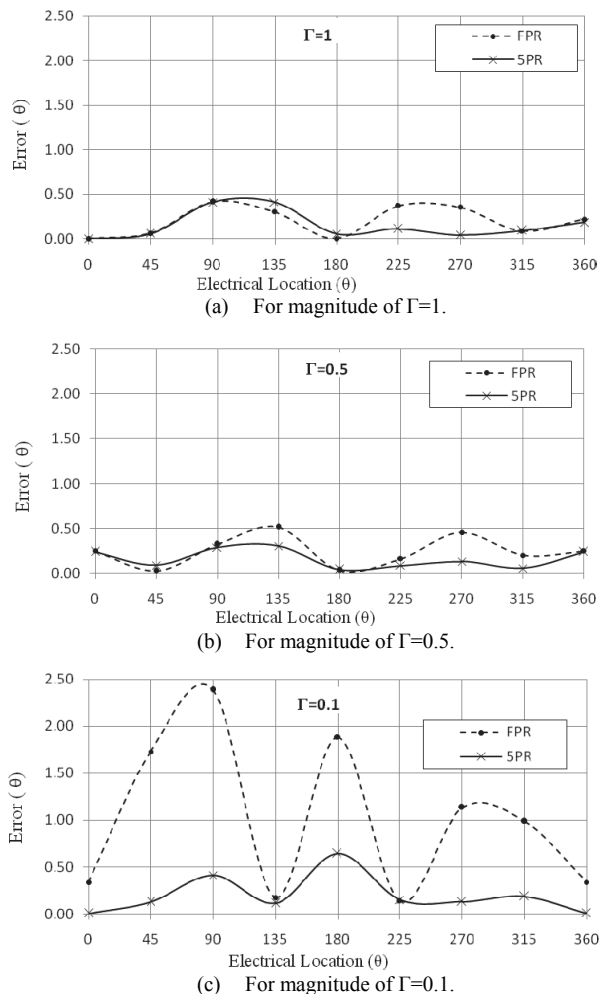


Fig. 7. Comparison of error in calculated phase-shifts.

Standard	VNA		FPR		5PR	
	Mag	P-shift	Mag	P-shift	Mag	P-shift
std1	0.9860	-30.30	0.9962	-30.89	0.9931	-31.22
std2	0.9990	-69.61	1.0231	-72.56	1.0070	-72.13
std3	0.9910	52.60	0.9726	50.85	0.9750	50.20
std4	0.3687	-125.77	0.3557	-123.52	0.3592	-126.82
std5	0.5623	108.46	0.5560	106.24	0.5576	107.06
std6	0.0867	37.12	0.0698	34.29	0.0767	35.99
std7	0.1762	-102.89	0.1674	-103.38	0.1690	-103.33
std8	0.0200	9.67	0.0321	10.50	0.0270	8.25

Tab. 1. Comparison of FPR, 5PR, and VNA results for several unknown samples.

Standard	Magnitude Error		Phase-shift Error	
	5PR	FPR	5PR	FPR
std1	0.0071	0.0102	0.92	0.59
std2	0.0080	0.0241	2.52	2.95
std3	0.0160	0.0184	2.40	1.75
std4	0.0095	0.0130	1.05	2.25
std5	0.0047	0.0063	1.40	2.22
std6	0.0100	0.0169	1.13	2.83
std7	0.0072	0.0088	0.44	0.49
std8	0.0070	0.0121	1.42	0.83

Tab. 2. Error analysis of FPR and 5PR compared to VNA for several unknown samples.

to 5PR measurement. The simpler model only requires two detection ports with three calibration standards.

## 6. Conclusions

In this paper, the modification of 5PR to FPR has been realized. The new FPR is not limited to a fixed phase-shift for the phase-shift delay between measurement ports. A simple model and computational algorithm for FPR has been developed. It was proven that FPR can perform as well as 5PR and commercial VNA. With the new model and calculation algorithm, magnitude and phase-shift can be determined easily. The reduction of detection ports and calibration standards make the FPR structurally simpler and cost effective compared to conventional SPR.

## Acknowledgments

This work was supported by the Universiti Tunku Abdul Rahman under the UTAR Research Fund (UTARRF/2014-C1/L05).

## References

- [1] TRUSHKIN, A. N. A measuring device of the complex reflection coefficient. In *IEEE 23rd International Crimean Conference Microwave and Telecommunication Technology (CriMiCo)*. Sevastopol (Ukraine), 2013, p. 963–964.
- [2] LEE, K., CHUNG, B., YOU, K., CHENG, E., ABBAS, Z. Study of dual open ended coaxial sensor system for calculation of phase

- using two magnitudes. *IEEE Journal on Sensors*, 2014, vol. 14, no. 1, p. 129–134. DOI: 10.1109/JSEN.2013.2281416
- [3] ENGEN, G. F. The six-port reflectometer: An alternative network analyzer. *IEEE Transactions on Microwave Theory and Techniques*, 1978, vol. 25, no. 12, p. 1075–1080. DOI: 10.1109/TMTT.1977.1129277
- [4] EROGLU, A., MADISHETTI, S. Six-port coupler design for high-power radio frequency applications. *IEEE Transactions on Instrumentation and Measurement*, 2014, vol. 63, no. 6, p. 1600–1612. DOI: 10.1109/TIM.2013.2289702
- [5] YEE, L. K., ABBAS, Z., JUSOH, M. A., YOU, Y. K., MENG, C. E. Determination of moisture content in oil palm fruits using a five-port reflectometer. *Sensors*, 2011, vol. 11, no. 4, p. 4073 to 4085. DOI: 10.3390/s110404073
- [6] GHANNOUCHI, F. M., MOHAMMADI, A. *The Six-Port Technique with Microwave and Wireless Applications*. Artech House, 2009. ISBN: 1608070336
- [7] BILIK, V. Six-port measurement technique: Principles, impact, applications. In *Proceedings of the International Conference Radioelektronika*. 2002.
- [8] ENGEN, G. F., HOER, C. A. Thru-reflect-line: An improved technique for calibrating the dual six-port automatic network analyzer. *IEEE Transactions on Microwave Theory and Techniques*, 1979, vol. 27, no. 12, p. 987–993. DOI: 10.1109/TMTT.1979.1129778
- [9] STASZEK, K., GRUSZCZYNSKI, S., WINCZA, K. Theoretical limits and accuracy improvement of reflection-coefficient measurements in six-port reflectometers. *IEEE Transactions on Microwave Theory and Techniques*, 2013, vol. 6, no. 8, p. 2966–2974. DOI: 10.1109/TMTT.2013.2269053
- [10] DVORAK, R., URBANEC, T. Data processing in multiport-based reflectometer systems. *Radioengineering*, 2011, vol. 20, no. 4, p. 832–837. DOI: 10.13164/re
- [11] HANSSON, E. R., RIBLET, G. P. An ideal six-port network consisting of a matched reciprocal lossless five-port and a perfect directional coupler. *IEEE Transactions on Microwave Theory and Techniques*, 1983, vol. 31, no. 3, p. 284–288. DOI: 10.1109/TMTT.1983.1131477
- [12] HADDADI, K., EL AABBAOUI, H., LOYEZ, C., GLAY, D., ROLLAND, N., LASRI, T. Wide-band 0.9 GHz to 4 GHz four-port receiver. In *IEEE International Conference on Electronics, Circuits and Systems*. Nice (France), 2006, p. 1316–1319. DOI: 10.1109/ICECS.2006.379724
- [13] HADDADI, K., WANG, M., GLAY, D., LASRI, T. Ultra wide-band four-port reflectometer using only two quadratic detectors. In *IEEE MTT-S International Conference: Microwave Symposium Digest*. 2008, p. 379–382. DOI: 10.1109/MWSYM.2008.4633182
- [14] HADDADI, K., WANG, M. M., NOURI, K., GLAY, D., LASRI, T. Calibration and performance of two new ultra-wideband four-port-based systems. *IEEE Transactions on Microwave Theory and Techniques*, 2008, vol. 56, no. 12, p. 3137–3142. DOI: 10.1109/TMTT.2008.2007138
- [15] HADDADI, K., WANG, M. M., GLAY, D., LASRI, T. Performance of a compact dual six-port millimeter-wave network analyzer. *IEEE Transactions on Instrumentation and Measurement*, 2011, vol. 60, no. 9, p. 3207–3213. DOI: 10.1109/TIM.2011.2124690
- [16] HADDADI, K., LASRI, T. Formulation for complete and accurate calibration of six-port reflectometer. *IEEE Transactions on Microwave Theory and Techniques*, 2012, vol. 6, no. 3, p. 574–581. DOI: 10.1109/TMTT.2011.2181861
- [17] DEB, K. *Multi-Objective Optimization using Evolutionary Algorithms*. John Wiley & Sons, 2001. ISBN: 978-0-471-87339-6

## About the Authors ...

**Kim Yee LEE** was born in 1978. He received his BSc Physics and Ph.D. degree from the Universiti Putra Malaysia in the year 2002 and 2008, respectively. His research interests include microwave measurement technique, microwave circuit and instrumentation, control and automation, dielectric measurement, microwave sensor and electromagnetic modeling.

**Boon Kuan CHUNG** received his B.Eng (Hons) in Electrical Engineering from the University of Malaya in 1992. He received his Ph.D. from Multimedia University in 2003. He is currently a Professor at the Department of Electrical and Electronic Engineering, Universiti Tunku Abdul Rahman. His research interests include microwave theory and techniques, antenna design, radar system, RCS calibrations, remote sensing, electromagnetic compatibility, wireless communication systems, and electronic instrumentation and measurements.

**Kok Yeow YOU** was born in 1977. He received the B.Sc. Physics in 2001 from Universiti Kebangsaan Malaysia, the M.Sc. degree in 2003, and the Ph.D. degree in 2006. His current research interests include theory, simulation, and instrumentation of electromagnetic wave propagation at microwave frequencies focusing on the development of microwave sensors for agricultural applications.

**Ee Meng CHENG** was born in 1980. He received the B.Sc. Instrumentation Science from Universiti Putra Malaysia in 2004, the M.Sc. in 2006, and the Ph.D. in 2009. His current research interests include computational electromagnetic modeling, microwave dielectric spectroscopy, and microwave sensors.

**Zulkifly ABBAS** was born in 1962. He received the B.Sc. Physics in 1986, the M.Sc. in 1994, and the Ph.D. from the University of Leeds in 2000. His current research interests include theory, simulation, and instrumentation of electromagnetic wave propagation at microwave frequencies focusing on the development of microwave sensors for agricultural applications.